

# Microwave Heating, Isothermal Sintering, and Mechanical Properties of Powder Metallurgy Titanium and Titanium Alloys

S.D. LUO, C.L. GUAN, Y.F. YANG, G.B. SCHAFFER, and M. QIAN

This article presents a detailed assessment of microwave (MW) heating, isothermal sintering, and the resulting tensile properties of commercially pure Ti (CP-Ti), Ti-6Al-4V, and Ti-10V-2Fe-3Al (wt pct), by comparison with those fabricated by conventional vacuum sintering. The potential of MW sintering for titanium fabrication is evaluated accordingly. Pure MW radiation is capable of heating titanium powder to  $\geq 1573$  K (1300 °C), but the heating response is erratic and difficult to reproduce. In contrast, the use of SiC MW susceptors ensures rapid, consistent, and controllable MW heating of titanium powder. MW sintering can consolidate CP-Ti and Ti alloys compacted from  $-100$  mesh hydride-dehydride (HDH) Ti powder to  $\sim 95.0$  pct theoretical density (TD) at 1573 K (1300 °C), but no accelerated isothermal sintering has been observed over conventional practice. Significant interstitial contamination occurred from the  $\text{Al}_2\text{O}_3$ -SiC insulation-susceptor package, despite the high vacuum used ( $\leq 4.0 \times 10^{-3}$  Pa). This leads to erratic mechanical properties including poor tensile ductility. The use of Ti sponge as impurity (O, N, C, and Si) absorbers can effectively eliminate this problem and ensure good-to-excellent tensile properties for MW-sintered CP-Ti, Ti-10V-2Fe-3Al, and Ti-6Al-4V. The mechanisms behind various observations are discussed. The prime benefit of MW sintering of Ti powder is rapid heating. MW sintering of Ti powder is suitable for the fabrication of small titanium parts or titanium preforms for subsequent thermomechanical processing.

DOI: 10.1007/s11661-012-1529-2

© The Minerals, Metals & Materials Society and ASM International 2012

## I. INTRODUCTION

HIGH-TEMPERATURE processing of materials by microwave (MW) radiation has emerged as a novel technique and shown promise for sintering, brazing, melting, heat treatment, and synthesis of a wide variety of materials including powder metals.<sup>[1–4]</sup> To date, MW sintering is an established process for ceramics and has been realized in industrial production. In contrast, MW sintering of powder metals is only a recent development,<sup>[5]</sup> but it has attracted increasing attention because of its potential for both cost reduction and property improvements.<sup>[5–9]</sup>

Magnetic and refractory powder metals appear to respond well to MW radiation compared with other powder metals which often show mild or weak responses.<sup>[10–13]</sup> Using the Heisenberg model, Tanaka *et al.*<sup>[14]</sup> have recently shown that MW radiation can heat magnetic metal oxides to temperatures well above their Curie temperatures while it is essentially ineffective for non-magnetic oxides. Their modeling identified that such fast heating “is caused by nonresonant response of electron spins in the unfilled  $3d$  shell to the wave magnetic field,”<sup>[14]</sup> and the effect “persists above the Curie temperature  $T_c$

because each electron spin is able to respond to the alternating magnetic field of MWs even above  $T_c$ .”<sup>[14]</sup> The same theory may apply to the MW heating and sintering of magnetic powder metals. The positive response of refractory powder metals to the MW radiation is not entirely surprising because these metals have a large covalent bonding component.<sup>[15]</sup>

Titanium alloys are advanced structural materials, but the high cost of titanium components has impeded their wider adoption for structural applications. A large proportion of the cost arises from the manufacturing process.<sup>[16]</sup> In this regard, powder metallurgy (PM) offers a promising route for both cost reduction and improved constitutional and microstructural capability for broad applications.<sup>[17,18]</sup> This makes MW heating and sintering particularly attractive, provided that the efficacy demonstrated on ceramics can be realized on titanium powder.

The current understanding of MW heating and sintering of titanium is summarized as follows:

- (a) *Response of titanium powder to MW heating* Pure MW radiation appears to be ineffective in heating titanium powder.<sup>[12,19]</sup> No fundamental reason has been proposed, but this may be attributed to titanium being a paramagnetic metal where only some spins of its unpaired  $3d$  electrons will be oriented by the external electromagnetic field<sup>[14]</sup> for limited magnetization.<sup>[20]</sup> Fortunately, the use of MW susceptors such as SiC can significantly enhance the heating efficacy.<sup>[21–25]</sup> Three mechanisms have been proposed to account for the effectiveness: heat radiation from the MW susceptors at low temperatures, the transformation of the MW-inert  $\text{TiO}_2$

S.D. LUO, Postdoctoral Research Fellow, C.L. GUAN, Ph.D. Candidate, Y.F. YANG, ARC Postdoctoral Research Fellow, G.B. SCHAFFER, Professor, and M. QIAN, Reader, are with The University of Queensland, School of Mechanical and Mining Engineering, ARC Centre of Excellence for Design in Light Metals, Brisbane, QLD 4072, Australia. Contact e-mail: ma.qian@uq.edu.au  
Manuscript submitted March 1, 2012.

Article published online November 13, 2012

film on each Ti powder particle to oxygen-deficient MW-absorbing Ti oxides, and the volumetric heating of Ti powder particles by eddy currents.<sup>[25]</sup> However, the consistency and capabilities of MW heating of titanium powder remain largely unknown.

- (b) *Sintering densification* Several studies on MW sintering of CP-Ti have indicated that the sintered density varies widely as a function of Ti powder size,<sup>[25]</sup> compaction pressure,<sup>[25]</sup> and isothermal sintering temperature.<sup>[22]</sup> The highest sintered density reported was ~96 pct theoretical density (TD) with fine Ti powder (<20  $\mu\text{m}$ , 0.70 wt pct oxygen), sintered at 1473 K (1200 °C) for 120 minutes.<sup>[25]</sup> No data are available on Ti alloys.
- (c) *Mechanical properties* To date, only two studies reported mechanical property data on MW-sintered CP-Ti and the results are discouraging. Hayashi<sup>[22]</sup> obtained an ultimate tensile strength (UTS) of  $\leq 275$  MPa and plastic strain ( $\epsilon_f$ ) of  $\leq 2.9$  pct. Kutty *et al.*<sup>[21]</sup> reported tensile strengths ranging from 140 to 410 MPa for MW-sintered CP-Ti samples which had a porous surface and a dense core. No ductility data were reported. Whether MW radiation is capable of producing attractive tensile properties for PM Ti and Ti alloys thus remains unanswered.

This study assesses the efficacy of MW heating, sintering densification, and as-sintered tensile properties of CP-Ti, Ti-6Al-4V, and Ti-10V-2Fe-3Al, compared with those fabricated by conventional vacuum sintering.

## II. EXPERIMENTAL PROCEDURE

CP-Ti, Ti-6Al-4V, and Ti-10V-2Fe-3Al were sintered. Table I lists the powder materials used in the current

study. Hydride-dehydride (HDH) Ti powder was sieved to three size ranges (<38, <45, and <63  $\mu\text{m}$ ), and the 66.7V-13.3Fe-20Al master alloy powder was sieved to two size ranges (75–150 and <38  $\mu\text{m}$ ). Powder mixtures were blended in a Turbula mixer for 30 minutes. Powder compaction was performed in a floating die under a uniaxial pressure. No lubricant was mixed in the powder nor was it applied to the die wall to avoid interstitial contamination and the effect of lubricant evaporation on temperature measurement. Table II lists the characteristics and usage of the powder compacts prepared. Thin rectangular bars (~2.5 g each) were pressed from Ti sponge to serve as impurity absorbers.

MW sintering was conducted in a 2.45 GHz 3 kW multi-mode applicator (HAMilab-HV3, Synotherm Co., Changsha, China) with an Al<sub>2</sub>O<sub>3</sub>-SiC insulation-susceptor package. Temperature was measured using an infrared pyrometer (MM2MH, Raytek Co., Santa Cruz, CA; 723 K to 2523 K (450 °C to 2250 °C), and emissivity 0.95). The cylindrical SiC susceptor weighs 145 g, and has dimensions of 70-mm inner diameter, 50-mm height, and 5-mm thickness. Firstly, comparative heating was conducted on CP-Ti cylinders with or without SiC susceptor, where one sample was heated in each run. Secondly, for the sintering of rectangular bars, four bars were positioned parallel to each other in the central region of the Al<sub>2</sub>O<sub>3</sub>-SiC insulation-susceptor package, spaced ~1 mm apart to avoid triggering sparks. Finally, green samples of CP-Ti and blended elemental (BE) Ti-10V-2Fe-3Al were MW-heated to 1573 K (1300 °C) at ~33 K/min (33 °C/min) and cooled to room temperature without any isothermal hold by switching off the MW input. The cooling time from 1573 K to 1273 K (1300 °C to 1000 °C) was ~8.5 minutes. The chamber was backed by a diffusion pump and kept at a vacuum  $\leq 4.0 \times 10^{-3}$  Pa throughout. Details about the furnace setup and the sintering parameters were reported

Table I. Powder Materials Used

Powder Product	Powder Purity (Mass Pct)	Particle Size ( $\mu\text{m}$ )	Supplier
Aluminum	99.0	30 to 300	AMPAL Inc., USA
Aluminum	99.7	<3	Aluminum Powder Company Ltd., UK
Master Alloy 42Al-58V	99.5	<150	Baoji Jia Cheng Rare Metal Materials Co. Ltd., China
Master Alloy 66.7V-13.3Fe-20Al	99.5	<150	Baoji Jia Cheng Rare Metal Materials Co. Ltd., China
Pre-Alloyed Ti-6Al-4V	99.5	106 to 150	Reading Alloys Inc., USA
HDH Ti Powder	99.4	<150	Kimet Special Metal Powder Co. Ltd., China
Ti Sponge	99.3	<2000	Kimet Special Metal Powder Co. Ltd., China

Table II. Characteristics of Titanium Powder Compacts and Usage

Sample Configuration	Compact Size (mm)	Alloy Composition	Compaction Pressure (MPa)	Usage
Cylinder	$\text{\O}20 \times 25$	CP-Ti, Ti-10V-2Fe-3Al, Ti-6Al-4V (BE, PA)	100	heating response
Rectangular Bar	$50 \times 8.2 \times 3$	CP-Ti	600, 750	sintering
		Ti-6Al-4V (BE)	600	densification & tensile test
		Ti-10V-2Fe-3Al	600	tensile test
	$55 \times 10 \times 2$	Ti Sponge	50	impurity getter

BE: Blended Elemental; PA: Pre-alloyed.

previously.<sup>[25]</sup> Conventional vacuum sintering was conducted at  $10^{-2}$  Pa in an Al<sub>2</sub>O<sub>3</sub> tube furnace which was heated and cooled at 4 K/min (4 °C/min) on account of the weak thermal shock resistance of the alumina furnace tube. Higher heating rates have no measurable effect on the densification of Ti.<sup>[26]</sup> Differential scanning calorimetry (DSC) (STA 409CD, Netzsch, Wittelsbacherstrasse, Germany) was used to analyze the thermal events in the powder compacts in flowing high-purity argon.

The green density was calculated from weight and dimensions, while the sintered density was measured by the Archimedes method.<sup>[25]</sup> Dog-bone like tensile specimens (2.7 mm × 3 mm cross section and 15-mm gauge length) were machined from sintered bars and tested at room temperature on an Instron tester (Model 5584, Instron Co., Norwood, MA) at a crosshead speed 0.5 mm/min. A video extensometer was used to record the displacement. Samples cut from tensile bars were polished and etched with Kroll's solution for metallographic examination by an optical microscope and a scanning electron microscope (SEM, XL 30, FEI Philips, Hillsboro, OR). Chemical analysis was conducted on a Leco TC-436 for oxygen (O) and nitrogen (N), and on a Leco CS-444 for carbon (C) (LECO Co., Michigan, US). The analysis of silicon (Si) was done on a Spectro ICP-OES09 (SPECTRO Analytical Instruments GmbH, Kleve, Germany).

### III. RESULTS

#### A. MW Heating Response

Figure 1 shows four heating curves of CP-Ti cylindrical samples obtained by MW radiation without the use of SiC MW susceptors. Pure MW radiation succeeded in heating the CP-Ti powder to 1573 K (1300 °C) in two trials (see curves 1 and 2). However, the heating process was not reproducible (*e.g.*, neither trial 3 nor

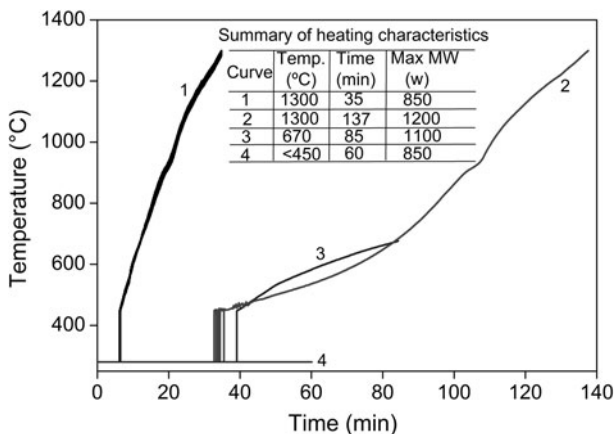


Fig. 1—Heating profiles of CP-Ti cylinders by MW radiation. MW power input: 300 W in the first 3 min, increased by 50 W every 3 min in the next 35 min, which afterward was adjusted according to MW reflection intensity.

trial 4 in Figure 1 was successful), and it showed clear spark discharging, often in the form of a hot spot.

Figure 2(a) shows the MW heating curves of CP-Ti with SiC susceptors under various MW power-input conditions. Heating rates ranging from 17 K/min to 50 K/min (17 °C/min to 50 °C/min) [averaged from 723 K to 1573 K (450 °C to 1300 °C)] were readily achieved. Samples were heated almost linearly to the sintering temperature [1573 K (1300 °C)] without thermal runaway. In addition, no spark discharge was observed. Heating rates >50 K/min (50 °C/min) were achieved in a few trials. However, this was not actively pursued because it was necessary to allow the volatile inclusions, predominantly chloride and hydride, to progressively escape from the titanium powder.<sup>[18,27]</sup>

Figure 2(b) shows the heating responses of BE Ti-6Al-4V, PA Ti-6Al-4V, and BE Ti-10V-2Fe-3Al. The consistent linear increase in temperature indicates that MW heating of CP-Ti and Ti alloys is controllable and predictable.

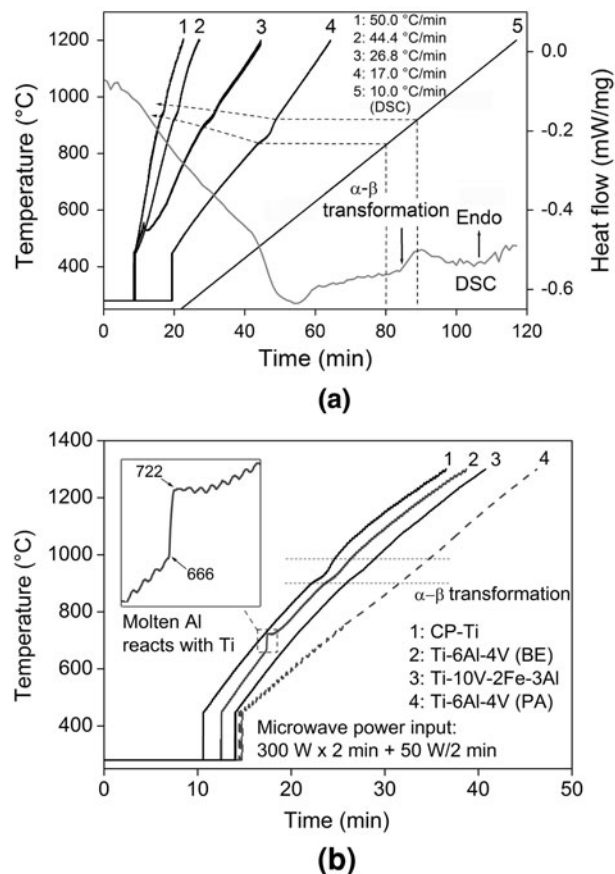


Fig. 2—(a) Microwave heating profiles with SiC susceptors recorded for powder compacts of CP-Ti with a superimposed DSC curve heated to 1573 K (1300 °C) at 10 K/min (10 °C/min). (b) Comparison of the MW heating profiles for powder compacts of CP-Ti, Ti-10V-2Fe-3Al, and Ti-6Al-4V at a heating rate of 32 K/min to 32.8 K/min (32 °C/min to 32.8 °C/min) (BE: blended elemental; PA: pre-alloyed). The isothermal holding stages were removed from each profile to focus on the heating stages.

**Table III. Heating Characteristics of Powder Compacts of CP-Ti, Ti-6Al-4V (BE), and Ti-10V-2Fe-3Al (BE) by Microwave Radiation (300 W Input in the First 2 Min and a Subsequent Augment of 50 W Every 2 Min)**

Sample Material	No.	Sample Mass (g)	Time to 723 K (450 °C) (min)	Time to 1573 K (1300 °C) (min)	Power to 1573 K (1300 °C) (W)	Heating Rate [RT–1573 K (1300 °C)] [K/min (°C/min)]	Reflected Power Fraction (Pct)	Temperature to Power Ratio* (°C/W)
CP-Ti	1	24	14	40	1300	31.9	10.5	1.0
	2	28	15	42	1300	30.4	9.5	1.0
	3	56	10	39	1250	32.9	15.3	1.04
Ti-6Al-4V	1	24	13	39	1250	32.7	7.4	1.04
	2	28	13	38	1250	33.6	9.5	1.04
Ti-10V-2Fe-3Al	3	56	10	38	1250	33.6	12.5	1.04
	1	24	12	40	1250	31.9	8.6	1.04
	2	28	15	40	1250	31.9	8.4	1.04
	3	56	10	37	1200	34.5	11.4	1.08

\*Referring to the sintering temperature [1573 K (1300 °C)] and the input MW power consumed on reaching 1573 K (1300 °C).

Table III lists in detail the MW heating characteristics of CP-Ti, BE Ti-6Al-4V, and BE Ti-10V-2Fe-3Al, where the MW power input was 300 W in the first 2 minutes, followed by an increment of 50 W every 2 minutes. The efficiency of MW heating is consistent and reproducible for each titanium composition evaluated. It is noted that the reflected MW power fraction is generally around 10 pct, giving an average temperature-to-input power ratio of 274 K/W ( $\geq 1.0$  °C/W).

### B. Sintered Density

Figure 3(a) shows the densities obtained from isothermal sintering of CP-Ti, BE Ti-6Al-4V, and BE Ti-10V-2Fe-3Al bars at 1573 K (1300 °C) by MW radiation with a SiC susceptor. The heating rate was set in the narrow range from 30 K/min to 33 K/min (30 °C/min to 33 °C/min). The initial 30-minute isothermal hold at 1573 K (1300 °C) resulted in low sintered densities for each composition: ~93.4 pct TD for CP-Ti, ~92.3 pct

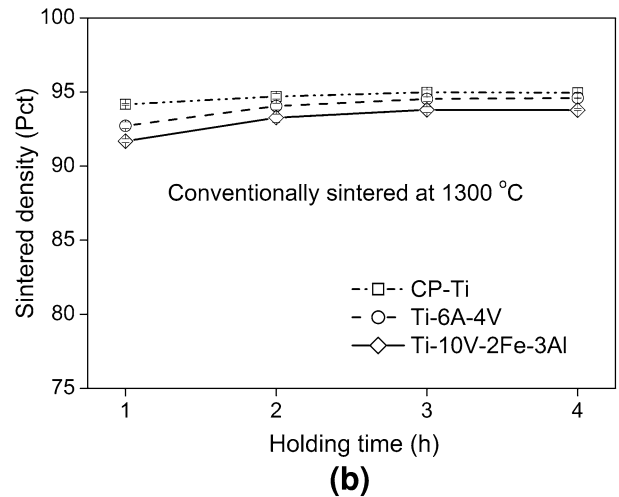
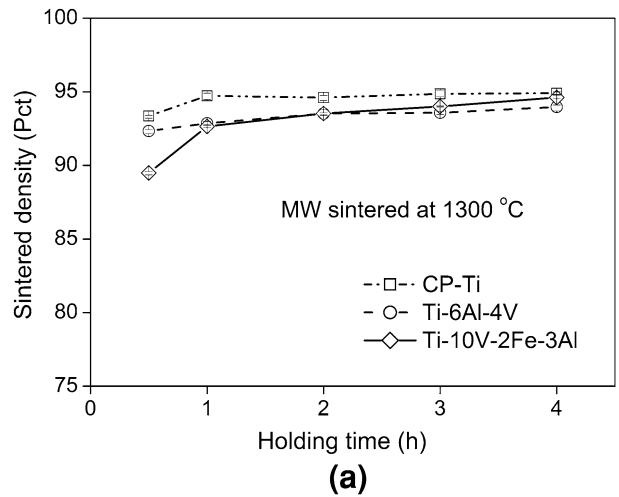


Fig. 3—Sintered densities of CP-Ti, BE Ti-6Al-4V, and Ti-10V-2Fe-3Al at 1573 K (1300 °C) as a function of isothermal hold time: (a) MW radiation with SiC susceptors, heating rate: 30 K/min through 32 K/min (30 °C/min to 32 °C/min), and (b) conventional vacuum sintering, heating rate: 4 K/min (4 °C/min). Samples were pressed at 600 MPa. Each data point is the average of four samples.

**Table IV. Impurities in MW-Sintered CP-Ti With and Without the Protection of Ti Sponge**

Package Design	Sample Location	O (ppm)	C (ppm)	N (ppm)	Si (ppm)	Mass Gain (Mass Percent)
No Protection	1 and 4 in Fig. 4	4500	560	210	350	0.54
	2 and 3 in Fig. 4	3000	360	140	280	0.23
Protection	1 and 4 in Fig. 4	2200	140	96	80	-0.05
	2 and 3 in Fig. 4	2100	160	93	100	-0.06
HDH Ti Powder		2000	80	77	73	

All samples were sintered from <150 μm Ti powder at 1573 K (1300 °C) for 2 h at a heating rate of 30 K/min to 32 K/min (30 °C/min to 32 °C/min).

TD for BE Ti-6Al-4V, and ~89.5 pct TD for BE Ti-10V-2Fe-3Al. A small increase occurred in the next 30 minutes, but thereafter the sintered density increased only slightly with increasing isothermal hold and reached ~95 pct TD after 240 minutes at 1573 K (1300 °C). The sintering densification occurred slowly at 1573 K (1300 °C). Figure 3(b) shows the results obtained from conventional vacuum isothermal sintering of the same titanium materials at 1573 K (1300 °C) with a heating rate of 4 K/min (4 °C/min). The observations are very similar.

**C. Tensile Properties**

*1. Effect of interstitial contamination*

The interstitial contamination in samples sintered at 1573 K (1300 °C) with and without the protection of Ti sponge is given in Table IV. Naked sintering produced high interstitial (O, N, C, and Si) contents and a weight gain ranging from 0.23 to 0.54 pct. In contrast, sintering under the protection of Ti sponge exerted little influence on the O and N contents. Pick-ups of C and Si did occur, but to a much lesser extent. There was also a minor mass loss under the protection of Ti sponge. The oxygen contents of the CP-Ti sintered at 1573 K (1300 °C) for 2 and 3 hours in the conventional vacuum sintering furnace under the protection of sponge are 0.20 and 0.22 pct, respectively. The C and N contents are both 0.01 pct. They are all similar to the MW sintered under the protection of titanium sponge.

Figure 4(a) shows the tensile properties and the sintered densities of the four MW-sintered CP-Ti samples without the protection of Ti sponge. Samples 1 and 4 (lower ductility) were close to the insulation-susceptor package while samples 2 and 3 (higher ductility) were in the central region of the package. Although the sintered density is essentially the same, the tensile properties are erratic, and the plastic strain is poor (<8 pct) for as-sintered CP-Ti. Figure 4(b) shows the tensile properties of the MW-sintered CP-Ti with the protection of Ti sponge. Consistent tensile properties were obtained, and the plastic strain increased substantially.

*2. Tensile property with controlled interstitial contamination*

Figure 5(a) compares the UTS vs plastic strain ( $\epsilon_f$ ) for the CP-Ti sintered by MW radiation and conventional vacuum heating. Also included are some literature data

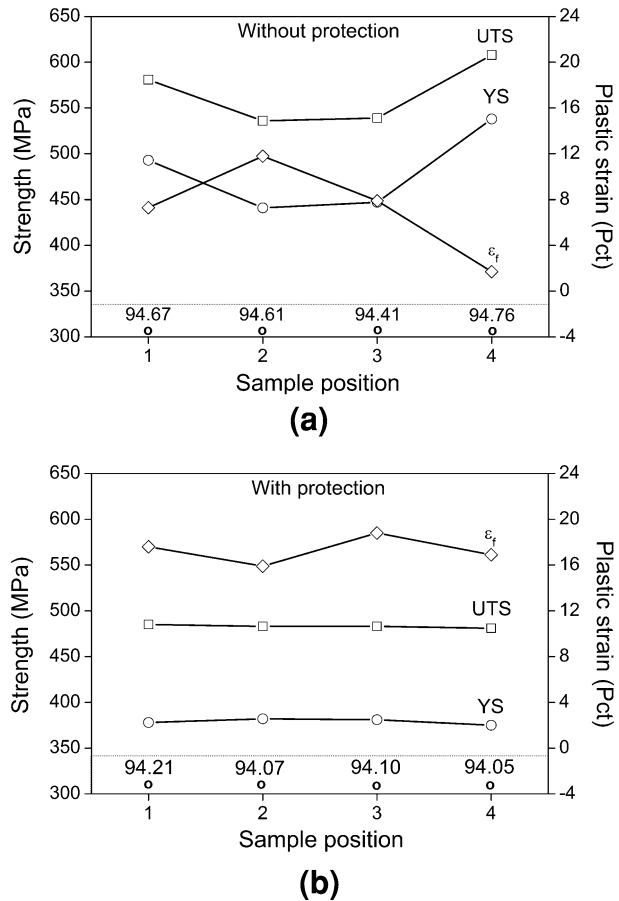


Fig. 4—Tensile properties of MW-sintered CP-Ti in relation to sample locations: (a) without the protection of Ti sponge and (b) with the protection of Ti sponge. Samples were pressed at 600 MPa and sintered at 1573 K (1300 °C) for 2 h with a heating rate ranging from 30 K/min to 32 K/min (30 °C/min to 32 °C/min) [averaged from 723 K to 1573 K (450 °C to 1300 °C)]. The figures given above the horizontal axis are the sintered densities. Samples 1 and 4 were close to the insulation-susceptor package; samples 2 and 3 were in the central region of the package.

and the ASTM property requirements for CP-Ti Grades 2 to 4. The tensile properties obtained from the use of -100 mesh (<150 μm) HDH Ti powder are UTS = 480–512 MPa and  $\epsilon_f$  = 15.0 through 21.3 pct. They are typical for CP-Ti fabricated by the conventional PM approach,<sup>[28]</sup> and fall within the range of ASTM Grades 2–4. However, it should be pointed out that the mechanical properties of the as-sintered CP-Ti and thus the capabilities of MW sintering are affected by

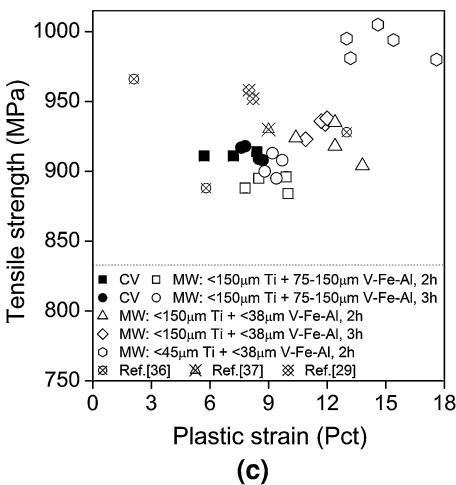
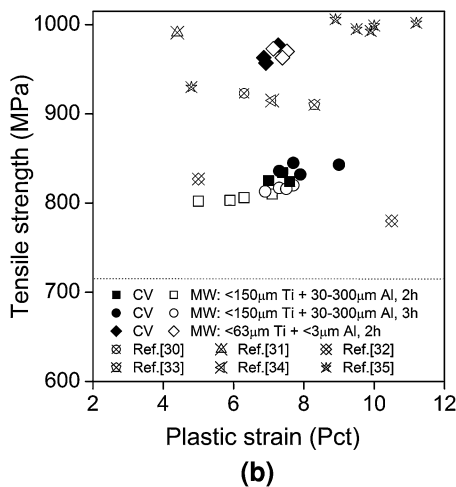
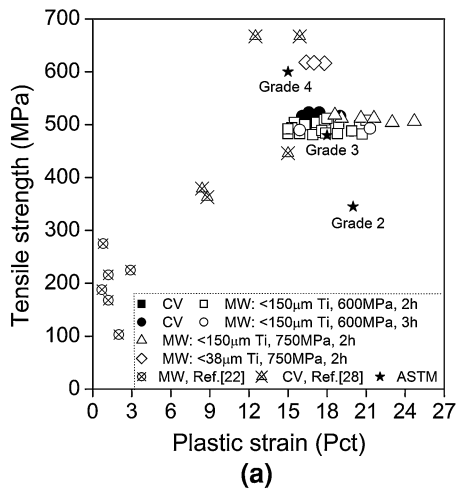


Fig. 5—Tensile property comparison between the MW-sintered and conventionally vacuum-sintered samples under different conditions. (a) CP-Ti; (b) Ti-6Al-4V, compacted from blends of elemental Ti and Al powders and Al-V master alloy powder (particle size  $<150\ \mu\text{m}$ ) at 600 MPa; and (c) Ti-10V-2Fe-3Al, compacted from blends of Ti powder and V-Fe-Al master alloy powder at 600 MPa. Isothermal sintering was performed at 1573 K (1300 °C) from 2 to 3 h under the protection of Ti sponge for both sintering processes. Literature data<sup>[29–37]</sup> are included for comparison, although they vary significantly. CV: conventional vacuum.

both the powder size and compaction pressure. For instance, the UTS and  $\epsilon_f$  were increased to values ranging from 504 to 518 MPa and 18.6 to 24.7 pct, respectively, with increasing compaction pressure ranging from 600 to 750 MPa. In addition, the UTS was further increased to values ranging from 616 to 618 MPa when finer Ti powder ( $<38\ \mu\text{m}$ ) was compacted at 750 MPa. However, the plastic strain dropped to values ranging from 16.4 to 17.8 pct.

The results obtained for Ti-6Al-4V are summarized in Figure 5(b) together with representative literature data. The powder size showed a clear influence too. MW sintering resulted in slightly lower tensile properties than conventional vacuum sintering with the use of  $<150\ \mu\text{m}$  Ti powder, a commercial grade of 30 to 300  $\mu\text{m}$  Al powder, and  $<150\ \mu\text{m}$  42Al-58V master alloy powder. However, MW sintering produced slightly better tensile properties than conventional vacuum sintering when finer Ti powder ( $<63\ \mu\text{m}$ ) and Al powder ( $<3\ \mu\text{m}$ ) were used with the same 42Al-58V master alloy powder.

Figure 5(c) shows the results obtained for Ti-10V-2Fe-3Al and representative literature data. In general, MW sintering led to slightly lower tensile strength but better ductility than conventional vacuum sintering with the use of  $<150\ \mu\text{m}$  Ti powder and 75 to 150  $\mu\text{m}$  66.7V-13.3Fe-20Al master alloy powder. However, the use of finer master alloy powder ( $<38\ \mu\text{m}$ ) or finer Ti powder ( $<45\ \mu\text{m}$ ) and finer master alloy powder ( $<38\ \mu\text{m}$ ) together resulted in much improved tensile strength and ductility by MW sintering. In particular, the  $\epsilon_f$  (13.0 to 17.6 pct) and UTS (980 to 1005 MPa) obtained from MW sintering of the powder blends of  $<45\ \mu\text{m}$  Ti and  $<38\ \mu\text{m}$  V-Fe-Al are much better than those achieved by conventional vacuum sintering of similar powder blends.<sup>[29]</sup> It has been shown that the key to the fabrication of BE Ti-10V-2Fe-3Al by sintering is to achieve a homogeneous microstructure.<sup>[29]</sup> The outstanding as-sintered plastic strain suggests that this has been achieved by MW sintering.

### 3. Microstructure and fractographs

Figure 6 shows the microstructures of CP-Ti and BE Ti-10V-2Fe-3Al heated to 1573 K (1300 °C) and cooled to room temperature without an isothermal hold by switching off MW input. Significant sintering necks were developed between the Ti particles during heating to 1573 K (1300 °C). Figure 7 shows the microstructures of the MW-sintered CP-Ti, Ti-6Al-4V Ti-10V-2Fe-3Al, and the corresponding tensile fractographs. Pores are visible in each case, corresponding to the sintered densities ranging from 94.5 to 95.5 pct TD. The fracture surfaces of both CP-Ti and Ti-10V-2Fe-3Al (Figures 7(d) and (f)) feature a large number of deep dimples, consistent with the plastic strain obtained. In addition, the CP-Ti samples showed serpentine dimple walls manifesting severe plastic deformation during tension. The as-sintered microstructure of Ti-6Al-4V is typical (Figure 7(b)), and its fracture surface (Figure 7(e)) confirms that its as-sintered microstructure is less ductile than the as-sintered CP-Ti and Ti-10V-2Fe-3Al.

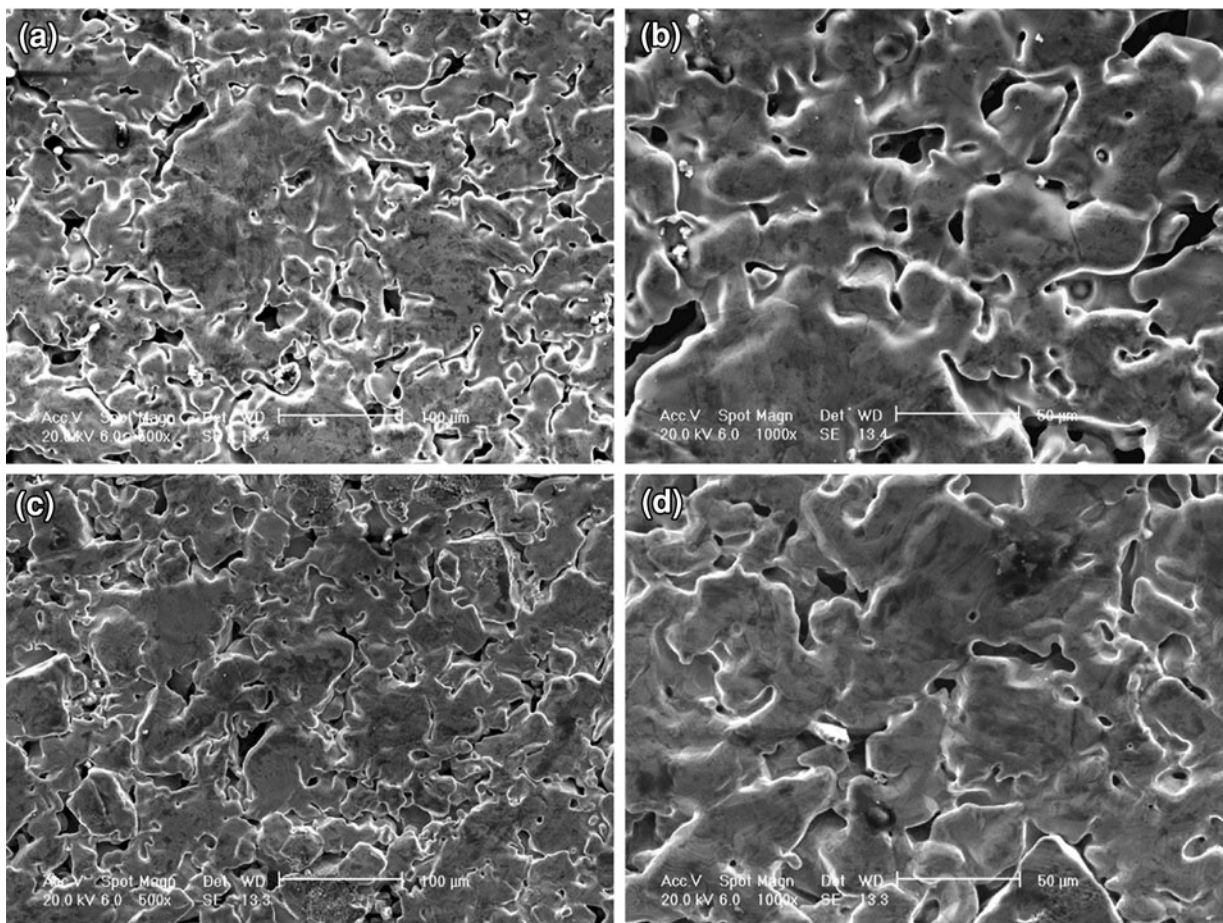


Fig. 6—Microstructures of CP-Ti and BE Ti-10V-2Fe-3Al powder compacts heated to 1573 K (1300 °C) by MW radiation and cooled to room temperature without an isothermal hold by switching off MW input. (a) and (b): CP-Ti, and (c) and (d): BE Ti-10V-2Fe-3Al. (b) and (d) are magnified views of (a) and (c), respectively. Significant sintering necks were developed between the Ti particles during heating to 1573 K (1300 °C) by MW radiation.

## IV. DISCUSSION

### A. Heating Response and MW Susceptor

The results shown in Figure 1 provide direct evidence that pure MW radiation can heat titanium powder to temperatures  $>1573$  K (1300 °C) but the heating process is not reproducible. It was noticed that there was clear spark discharging (often in the form of hot spot) without the use of MW susceptors. Continuous spark discharging can heat the titanium powder to an elevated temperature, up to  $\sim 1073$  K (800 °C). However, it causes inconsistent and uncontrollable heating and even thermal runaway. At temperatures  $>1073$  K (800 °C), the MW-inert  $\text{TiO}_2$  film on each Ti powder particle will transform to MW-absorbing oxygen-deficient  $\text{TiO}_x$  ( $x < 2$ ) oxides, as a result of oxygen diffusing into the titanium metal. This favors MW heating. In addition, the volumetric heating of Ti powder particles by eddy currents<sup>[25]</sup> intensifies with increasing temperature because of the increased electrical resistivity. These combined effects resulted in MW heating of Ti powder to  $\geq 1573$  K (1300 °C). However, pure MW radiation without susceptors is not always effective, for reasons that remain unidentified.

In contrast, the use of MW susceptors ensures consistent and controllable heating of titanium powder (Figure 2); no failure has been observed. The role of MW susceptors has been discussed previously.<sup>[25]</sup> MW susceptors provide a practical solution to the MW heating of titanium powder.

The MW heating curves obtained with the use of susceptors show a number of features. The small temperature fluctuations shown on each curve in Figure 2(a) between  $\sim 1123$  K and  $\sim 1223$  K (850 °C and 950 °C) were caused by the  $\alpha$ - $\beta$  transformation of titanium, which is an endothermic process. This is supported by the DSC curve superimposed on Figure 2(a) for CP-Ti obtained at a heating rate of 10 K/min (10 °C/min). The noticeable temperature jump at  $\sim 943$  K (670 °C) observed on the heating curve of the BE Ti-6Al-4V in Figure 2(b) was close to the melting point of Al, but it was not caused by the melting of Al. An exothermic reaction starting at 928 K (655 °C) was confirmed by a separate DSC analysis. Leitner *et al.*<sup>[38]</sup> reported similar observations in heating Ti-Al powder blends. Their analyses identified that the temperature change corresponded to the formation of  $\text{TiAl}_3$  because of the reaction between molten Al and Ti.

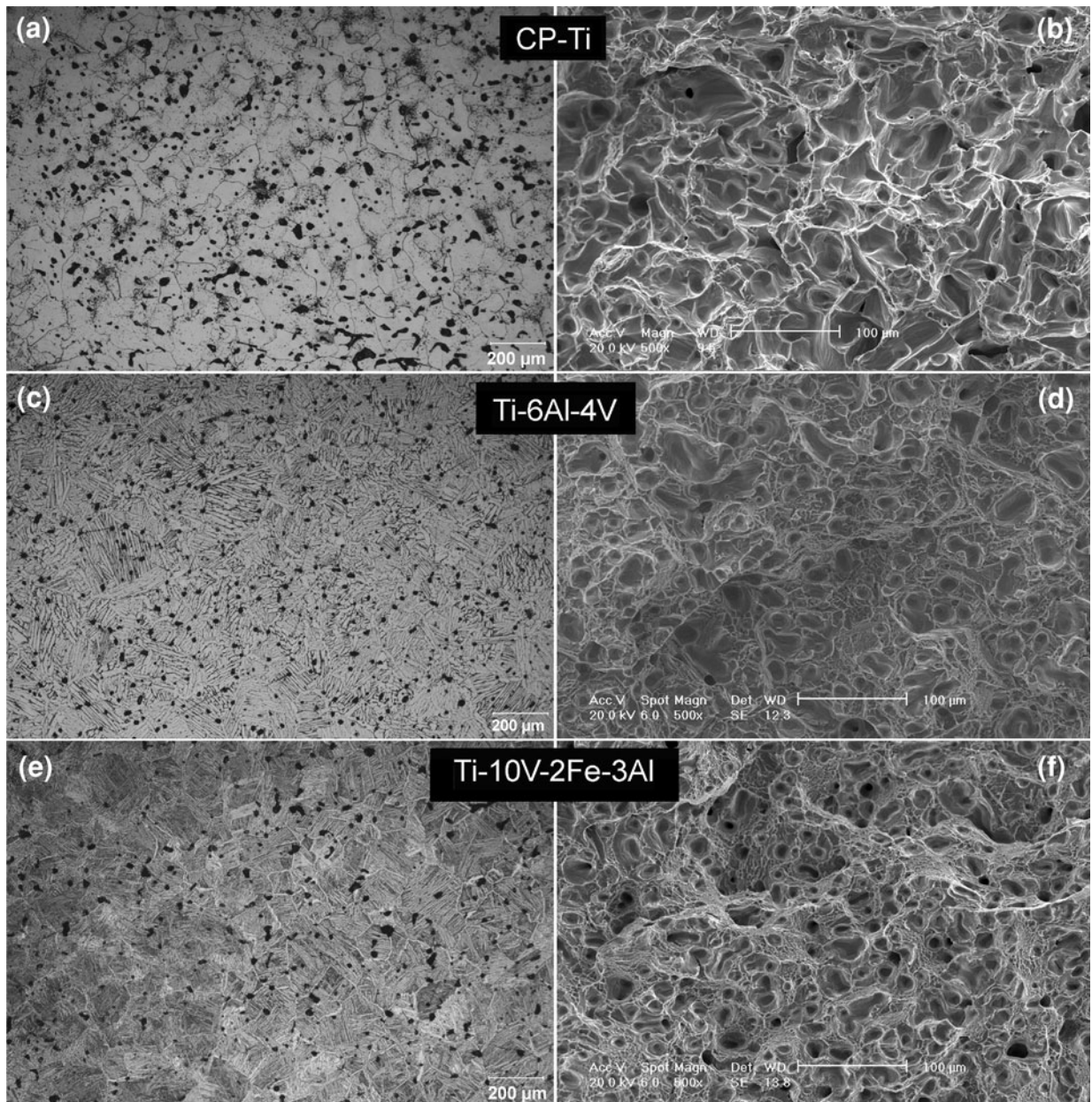


Fig. 7—MW-sintered CP-Ti ( $<150 \mu\text{m}$  Ti), Ti-6Al-4V ( $<63 \mu\text{m}$  Ti, 75-150  $\mu\text{m}$  Al-V, 3  $\mu\text{m}$  Al), and Ti-10V-2Fe-3Al ( $<45 \mu\text{m}$  Ti,  $<38 \mu\text{m}$  V-Fe-Al). (a-c) are optical micrographs (etched) while (d-f) are the corresponding SEM tensile fractographs. Samples were pressed at 600 MPa, and sintered at 1573 K (1300 °C) for 2 h.

### B. Sintering Densification

The systematic study shown in Figure 3 revealed no advantages of MW sintering over conventional vacuum sintering in terms of densification. Detailed analysis was then made of the microstructure of CP-Ti and BE Ti-10V-2Fe-3Al which were MW heated to 1573 K (1300 °C) and cooled to room temperature without an isothermal hold. We assume that there was little further sintering during cooling from 1573 K (1300 °C) to room temperature.

Metallographic examination showed that samples all exhibited noticeable shrinkage, with the relative density increasing from 82.6 pct TD to 86.8 pct TD for CP-Ti and from 78.0 pct TD to 84.8 pct TD for BE Ti-10V-

2Fe-3Al. Sintering necks were developed between the powder particles during heating to 1573 K (1300 °C) by MW radiation, leading to well-interconnected particles (see Figures 6(b) and (d)). These sintering necks enable the free electrons to move between the titanium particles and therefore effectively transform the sample into a bulk form, although it is still porous. It has been shown that the inter-particle bonding developed during sintering can substantially increase the electrical conductivity of metal powder compacts<sup>[39,40]</sup> even though the relative density of the titanium powder compacts is only about 90 pct TD.<sup>[40]</sup> This is a fundamental change from the green state which is an aggregate of compacted powder



particles. Because of this change, the eddy currents produced by the alternating magnetic field of the incident MWs can readily develop in the entire skin layer, and this in turn will generate an alternating magnetic field around the surface with its B vector being opposite to that of the incident MWs.<sup>[12]</sup> This opposite “reflected” wave can largely weaken or even cancel out the incident MWs, limiting the interactions to the skin layer.<sup>[12]</sup> In this state, the heat generated from the interactions will transfer inward from the surface to the interior, in the same fashion as conventional sintering. This leads to similar sintering kinetics between the MW and conventional vacuum sintering. As a result, the advantages of MW sintering of titanium powder are mainly restricted to the heating stage.

### C. Interstitial Contamination During MW Sintering

The mechanical properties of titanium are sensitive to the interstitial content. Substantial interstitial contamination occurred during MW sintering (see Table IV), corresponding to the erratic tensile properties shown in Figure 4(a). Given the high vacuum conditions ( $\leq 4.0 \times 10^{-3}$  Pa) used for MW sintering, the Al<sub>2</sub>O<sub>3</sub>-SiC insulation-susceptor package can be assumed to be the main source of interstitial contamination. This is supported by the noticeable increase in the Si content of the samples sintered without titanium sponge protection (see Table IV). The stability of Al<sub>2</sub>O<sub>3</sub> and SiC at 1573 K (1300 °C) in high vacuum under intense MW radiation is unknown. However, the noticeable pick-up of Si from 73 ppm in the HDH Ti powder to values ranging from 280 to 350 ppm in the as-sintered CP-Ti suggests that some decomposition of SiC may have occurred.

The insulation-susceptor package is critical to ensure rapid and consistent MW heating. The use of other insulation package materials to reduce the interstitial contamination was considered. In theory, ceramics that are transparent to MWs such as ZrO<sub>2</sub>, Y<sub>2</sub>O<sub>3</sub>, and BN are all effective candidate materials. Table V compares the physical properties and prices of several ceramics and their inertness to SiC. Al<sub>2</sub>O<sub>3</sub> is advantageous over the other three in terms of its weak interaction with MWs (loss tangent) at temperatures up to 1073 K (800 °C). More importantly, the affordability and availability make Al<sub>2</sub>O<sub>3</sub> a material of choice as an insulation consumable. SiC has similar advantages over ferrites and MoSi<sub>2</sub> as MW susceptors. This explains why the Al<sub>2</sub>O<sub>3</sub>-SiC package is the most commonly used combination for MW sintering of Ti and other metals.

The placement of pressed Ti sponge adjacent to the test samples during sintering effectively eliminated interstitial contamination (Table IV), producing consistent tensile strength and substantially improved plastic strain. Experiments have shown that the Ti sponge getter remains effective after >20 sintering trials at 1573 K (1300 °C) in high vacuum ( $\leq 4.0 \times 10^{-3}$  Pa).

### D. Assessment of MW Sintering for PM Titanium

MW sintering is capable of producing good tensile properties for both CP-Ti and Ti alloys with the assistance of MW susceptors and effective control of interstitial contamination using Ti sponge (Figure 5). The as-sintered microstructures (Figures 7(a–c)) are typical of those conventionally sintered, and the fractographs (Figures 7(d–f)) are consistent with the plastic strain demonstrated. The use of SiC MW susceptors ensures consistent and reliable MW heating. SiC is inexpensive, and a SiC susceptor is still effective after more than 100 sintering runs. Despite the lack of accelerated isothermal sintering over conventional practice, MW sintering can still considerably reduce the overall sintering cycle time. Figure 8 shows the difference recorded on laboratory trails. Given that MW heating does not produce fully dense titanium materials but significantly reduces the thermal cycle time, the process may be best exploited in the fabrication of preforms for subsequent thermomechanical processing or small titanium parts.

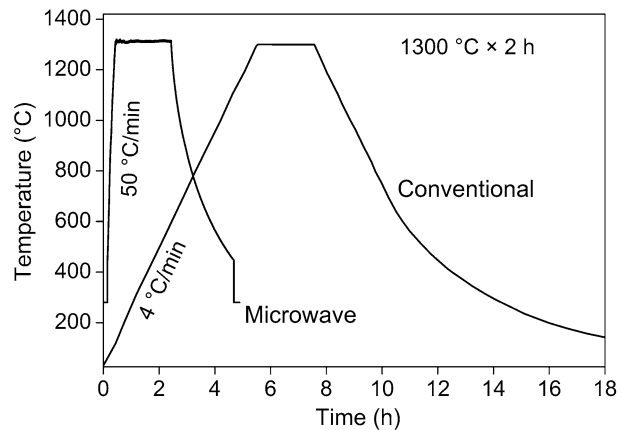


Fig. 8—Comparison of MW sintering and conventional vacuum sintering cycles.

Table V. Comparison of Commonly Used Insulation Materials Transparent to Microwaves

	Al <sub>2</sub> O <sub>3</sub>	ZrO <sub>2</sub>	Y <sub>2</sub> O <sub>3</sub>	BN
Price (\$/kg)	low	middle	high	high
Thermal Conductivity (W/m K)	30	1.7	27	3
Melting Point [K (°C)]	2345 (2072)	2988 (2715)	2698 (2425)	3246 (2973)
Loss Tangent	0.0001	0.0007	NA	0.003
Threshold Temperature Absorbing MW [K (°C)]	1073 (800)	673 (400)	NA	1023 to 1073 (750 to 800)
Reaction with SiC	yes	yes	yes	no

## V. CONCLUSIONS

1. The use of SiC MW susceptors is necessary to ensure consistent and reproducible heating of titanium powder. The MW heating curves recorded showed clear features of the  $\alpha$ - $\beta$  transformation and chemical reactions that occurred during heating.
2. The densities of CP-Ti, Ti-6Al-4V, and Ti-10V-2Fe-3Al compacted from -100 mesh HDH Ti powder at 600 MPa reached ~95.0 pct TD after sintering at 1573 K (1300 °C) for duration up to 3 hours by MW radiation. MW heating can significantly reduce the thermal cycle time. However, no advantages of isothermal sintering over conventional vacuum isothermal sintering were observed because the Ti powder compacts had essentially transformed into bulk form on reaching the sintering temperature.
3. MW sintering can be used to fabricate CP-Ti, Ti-6Al-4V, and Ti-10V-2Fe-3Al with tensile properties similar to or better than those of conventionally sintered titanium materials. The resulting mechanical properties are affected by both the powder size and compaction pressure.
4. Interstitial contamination from the Al<sub>2</sub>O<sub>3</sub>-SiC insulation-susceptor package occurred at 1573 K (1300 °C) during MW sintering. This led to erratic mechanical properties. However, the use of Ti sponge protection during sintering can eliminate the contamination and ensure good mechanical properties.

## ACKNOWLEDGMENTS

This study was supported by the Australian Research Council (ARC) through the Centre of Excellence for Design in Light Metals.

## REFERENCES

1. E. Siores and D. Do Rego: *J. Mater. Proc. Technol.*, 1995, vol. 48, pp. 619–25.
2. D.E. Clark and W.H. Sutton: *Annu. Rev. Mater. Sci.*, 1996, vol. 26, pp. 299–331.
3. Yu.V. Bykov, K.I. Rybakov, and V.E. Semenov: *J. Phys. D Appl. Phys.*, 2001, vol. 34, pp. 55–75.
4. D. Agrawal: *Trans. Indian Ceram. Soc.*, 2006, vol. 65, pp. 129–44.
5. R. Roy, D. Agrawal, J.P. Cheng, and S. Gedevisanishvili: *Nature*, 1999, vol. 399, pp. 668–70.
6. M. Gupta and W.W. Leong: *Microwaves and Metals*, Wiley (Asia), Singapore, 2007.
7. N. Yoshikawa: *J. Microwave Power EE*, 2010, vol. 44, pp. 4–13.
8. A. Mondal: *Microwave Sintering of Metals*, LAP Lambert Academic Publishing, Saarbrücken, 2011.
9. G. Sethi, A. Upadhaya, and D. Agrawal: *Sci. Sinter.*, 2003, vol. 35, pp. 49–65.
10. P. Mishra, G. Sethi, and A. Upadhaya: *Metall. Mater. Trans. B*, 2006, vol. 37B, pp. 839–45.
11. M. Jain, G. Skandan, K. Martin, K. Cho, B. Klotz, R. Dowding, D. Kapoor, D. Agrawal, and J. Cheng: *Int. J. Powder Metall.*, 2006, vol. 42, pp. 45–50.
12. V.D. Buchelnikov, D.V. Louzguine-Luzgin, G. Xie, S. Li, N. Yoshikawa, M. Sato, A.P. Anzulevich, I.V. Bychkov, and A. Inoue: *J. Appl. Phys.*, 2008, vol. 104, p. 113505.
13. A. Mondal, D. Agrawal, and A. Upadhaya: *J. Microwave Power EE*, 2010, vol. 44, pp. 28–44.
14. M. Tanaka, H. Kona, and K. Maruyama: *Phys. Rev. B*, 2009, vol. 79, p. 104420.
15. M.F. Ashby and D.R.H. Jones: *Engineering Materials 1: An Introduction to their Properties, Applications and Design*, 4th ed., Butterworth-Heinemann, Oxford, 2011, p. 58.
16. M.A. Imam, F.H. Froes, and K.L. Housley: *Kirk-Othmer Encyclopedia of Chemical Technology*, Wiley, New York, 2010, pp. 1–41.
17. F.H. Froes and D. Eylon: *Int. Mater. Rev.*, 1990, vol. 35, pp. 162–68.
18. M. Qian: *Int. J. Powder Metall.*, 2010, vol. 46, pp. 29–44.
19. M. Sato, H. Fukusima, F. Ozeki, T. Hayasi, Y. Satito, and S. Takayama: *2004 Joint 29th International Conference on Infrared and Millimeter Waves and 12th International Conference on Terahertz Electronics*, Karlsruhe, 2004, pp. 831–32.
20. A. Cottrell: *An Introduction to Metallurgy*, 2nd ed., IOM, London, 1975, p. 495.
21. M.G. Kutty, S. Bhaduri, and S.B. Bhaduri: *J. Mater. Sci.: Mater. Med.*, 2004, vol. 15, pp. 145–50.
22. T. Hayashi: *Reports of Research Institute of Industrial Products Technology*, Research Institute Industrial Products Technology, Gifu, 2005.
23. T. Marcelo, J. Mascarenhas, and F.A.C. Oliveira: *Mater. Sci. Forum*, 2010, vols. 636–637, pp. 946–51.
24. R.W. Bruce, A.W. Fliflet, H.E. Huey, C. Stephenson, and M.A. Imam: *Key Eng. Mater.*, 2010, vol. 436, pp. 131–40.
25. S.D. Luo, M. Yan, G.B. Schaffer, and M. Qian: *Metall. Mater. Trans. A*, 2011, vol. 42A, pp. 2466–74.
26. I.M. Robertson and G.B. Schaffer: *Powder Metall.*, 2009, vol. 52, pp. 225–32.
27. S.D. Hill and R.V. Mrazek: *Metall. Trans.*, 1974, vol. 5A, pp. 53–58.
28. D.F. Heaney and R.M. German: in *Proceedings of the PM 2004 Powder Metallurgy World Congress*, H. Danninger and R. Ratzl, eds., European Powder Metallurgy Association, Shrewsbury, 2004, pp. 222–27.
29. Y.F. Yang, S.D. Luo, G.B. Schaffer, and M. Qian: *Mater. Sci. Eng. A*, 2011, vol. 528, pp. 6719–26.
30. T. Saito: *Adv. Perform. Mater.*, 1995, vol. 2, pp. 121–44.
31. Y. Yamamoto, J.O. Kiggans, M.B. Clark, S.D. Nunn, A.S. Sabau, and W.H. Peter: *Key Eng. Mater.*, 2010, vol. 436, pp. 103–11.
32. S. Abkowitz, J.M. Siergiey, and R.D. Regan: in *Modern Developments in Powder Metallurgy*, H.H. Hausner, ed., Metal Powder Industries Federation, Princeton, 1971, pp. 501–11.
33. A.D. Hanson, J.C. Runkle, R. Widmer, and J.C. Hebeisen: *Int. J. Powder Metall.*, 1990, vol. 26, pp. 157–64.
34. F.H. Froes, S.J. Mashl, V.S. Moxson, J.C. Hebeisen, and V.A. Duz: *JOM*, 2004, vol. 56, pp. 46–48.
35. O.M. Ivasishin, D.G. Savvakina, I.S. Bielov, V.S. Moxson, V.A. Duz, R. Davies, and C. Lavender: in *Proceedings of Conference on Science and Technology of Powder Materials: Synthesis, Consolidation and Properties*, Pittsburgh, MS&T 2005, pp. 151–58.
36. N.R. Moody, W.M. Garrison, Jr., J.E. Smugeresky, and J.E. Costa: *Metall. Trans. A*, 1993, vol. 24A, pp. 161–74.
37. H. Guo, Z. Zhao, C. Duan, and Z. Yao: *JOM*, 2008, vol. 60, pp. 47–49.
38. G. Leitner and K. Jaenicke-Ressler: *J. Phys. IV*, 1993, vol. 3, p. 403.
39. J. Ma, J.F. Diehl, E.J. Johnson, K.R. Martin, N.M. Miskovsky, C.T. Smith, G.J. Weisel, B.L. Weiss, and D.T. Zimmerman: *J. Appl. Phys.*, 2007, vol. 101, p. 074906.
40. Yu.N. Podrezov, V.A. Nazarenko, A.V. Vdovichenko, V.I. Danilenko, O.S. Koryak, and Ya.I. Evich: *Powder Metall. Metal Ceram.*, 2009, vol. 48, pp. 201–10.